Power System Protection and Control
ISSN:1674-3415

AUTONOMOUS CONTROL OF VARIABLE SPEED THREE PHASE INDUCTION MOTOR DRIVE FOR EV/AERO-SPACE APPLICATIONS

Chandra Shekar S M[1], Reddy Sudharshana K[2], Prakash S Ari[3], Shameer N[4], A Ramachandran[5]

[1]Dept. of ECE, Vemana Institute of Technology, VTU, Bengaluru, India. smcvit16@gmail.com, https://orchid.org/0009-0005-7619-0538
[2]Dept. of ECE, Vemana Institute of Technology, VTU, Bengaluru, India. reddy3690@gmail.com, https://orchid.org/0000-0001-8963-359X
[3]Dept. of ECE, Vemana Institute of Technology, VTU, Bengaluru, India. prakashsari2012sr@gmail.com, https://orcid.org/0009-0008-8593-8116
[4]Electric Power Train, BlueBinaries Engineering and Pvt Ltd., Bengaluru, India. shameer.nkth@gmail.com, https://orcid.org/0009-0005-6944-0674
[5]Dept. of ECE, Vemana Institute of Technology, VTU, Bengaluru, India. arama1947@gmail.com, https://orcid.org/0009-0006-8434-0628
*Corresponding Author: 1smcvit16@gmail.com

Received: 14/05/2026 **Revised**: 18/06/2026 **Accepted**: 25/07/2026

***ABSTRACT*:**

Induction motor drives are widely used in variable speed for electric vehicles, aerospace control applications. Due to advances in power-electronic switching devices, it is possible to control the speed of an induction motor. The microcontrollers are programmed with a unit sine curve for the 1st 256 locations. By addressing the microcontroller at different speeds, various sine-frequency outputs can be generated. Since the microcontroller's output is digital, an appropriate digital to analog converter is used to get sine wave. This voltage is being modulated with a high carrier frequency. A comparator compares the pulse width modulation output with the feedback voltage from the current transformer motor terminals. This comparator output is given to the D-flip-flop to get 2 complementary outputs for the inverter legs. Similarly, for all 3 phases, control voltages are generated, and the outputs are passed through appropriate dead-zone generators, which are then applied to the MOSFET gates. Suitable opto-couplers are used to isolate the control signal from high voltages. The inverter output is given to the motor terminals. Current Transformers are used for each phase and fed back to the comparator for control purposes. The system has been tested for various frequencies from 30 - 62.5Hz. The mixed signal oscilloscope records the phase, line voltages across motor terminals and the snubber inductor waveforms in bitmap and csv format. The csv format is used to do FFT analysis to get frequency domain results to identify fundamental and higher harmonic frequency voltages present in the phase and line voltages. The higher harmonic components voltage may produce negative torque in the motor, hence it is necessary to identify. The result shows that there is no overshoot at the terminal voltage of phase and line in all the speeds of induction motor due to proper snubber circuits.

Keywords: *Fast Fourier Transformation. Induction Motor, Pulse Width Modulation, Sine Modulation.*

INTRODUCTION

The block diagram of the control system for running the 3-phase IM is shown in Fig.1. The diagram contains electronic control circuit, opto-isolation and Current Transformer (CT) with disc type ferrite core, since high frequency currents are involved this type of core is used. The IM was run at 30, 40, 50, 60, and 62.5Hz frequencies at DC bus voltage 370V to the inverter bridge. The terminal voltage at motor terminal is recorded in BMP and CSV format in the (MSO) mixed signal oscilloscope [6]. The CSV results can be used to do signal analysis by using origin software. By using the math function the FFT waveform are also recorded. The detailed description is given in the following subdivision.

 DOI: 10.46121/pspc.54.3.32

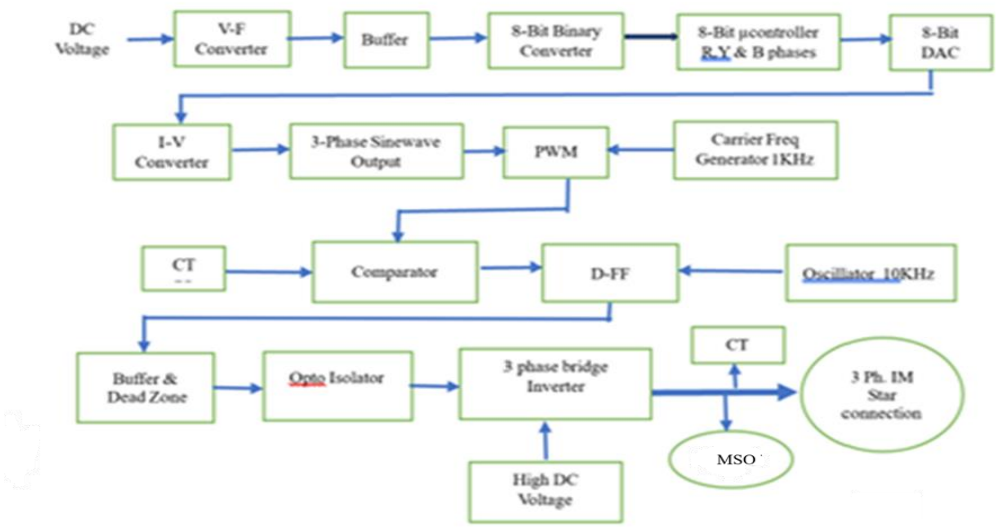

Fig.1 Induction motor variable-speed drive system block diagram.

METHODOLOGY

V-F Converter

The precision voltage to frequency converter Ic ideally suited for analogue-to-digital conversion. The output of a voltage-to-frequency converter is a pulse train whose frequency is precisely proportional to the applied input voltage. Thus, it provides all the inherent advantages of voltage-to-frequency conversion techniques [1],[2] and is easy to apply across standard voltage-to-frequency applications. The device's transfer function is (-10V), which gives a frequency 100 kHz.

Buffer

The voltage-to-frequency output voltage is buffered using the NPN transistor with a collector voltage of +5V, since this signal is fed to the two 4-bit binary counter ICs. Since it is buffered, it can be comfortably connected to two binary counters.

4-bit Binary Counter

This IC is a 4-bit binary ripple counter (mod-16) that counts from 0 to 15 (0000 to 1111 in binary). It consists of a divide-by-two and a divide-by-eight counter, enabling various counting modes, including Mod-16, via cascading, and features asynchronous master reset. By cascading the two 4-bit binary counter ICs, the 8-bit address from A_0 to A_7 is generated. The 8-bit waveform is shown in the Fig.2 (a).

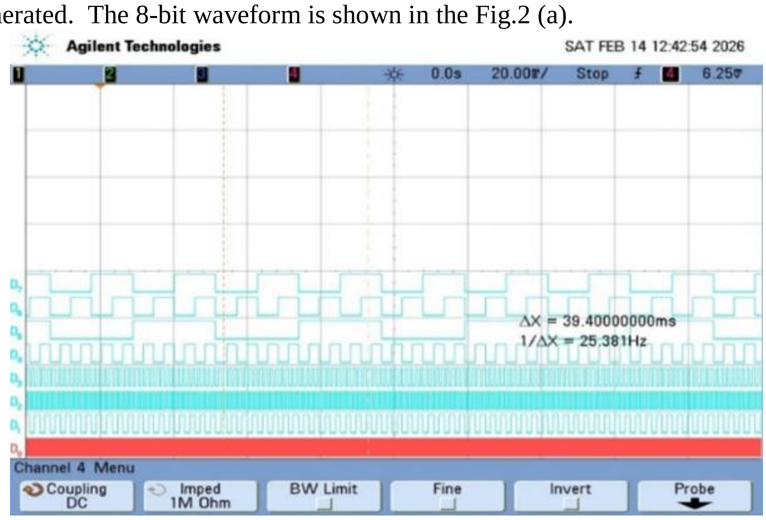

Fig. 2(a). 8-bit wave form of D_0 to D_8.

DOI: 10.46121/pspc.54.3.32

Microcontroller

The PIC 8-bit microcontroller is used in this project. One 10MHz crystal is connected to the appropriate terminals. Capacitor 0.1µF is connected between +5V and ground as a filter capacitor. Pull-up resistor of 10kΩ, connected at the corresponding terminals to +5V. The address lines from binary counter connected as A_0 to A_3 to at the address terminals. The microcontroller is embedded with a unit sine curve in hex format for the first 256 locations for the R phase, and similarly for the Y and the B phase across three separate microcontrollers. All the three microcontrollers are given the same address lines of A_0 to A_7. By increasing or decreasing the address speed (A_0 to A_7) the frequency of the sine waveform in digital output proportionally can be increased or decreased [1].

Digital to Analog converter

The 8-bit DAC is used for converting the digital signals from the microcontroller to an analog signal. The DAC signals are current outputs that are converted to voltage signals using an OP-AMP. Three such DAC is used for the three microcontrollers for R, Y and B phases [4]. The three OP-AMP output phase voltages are shifted by 120° which is shown in Fig.2 (b).

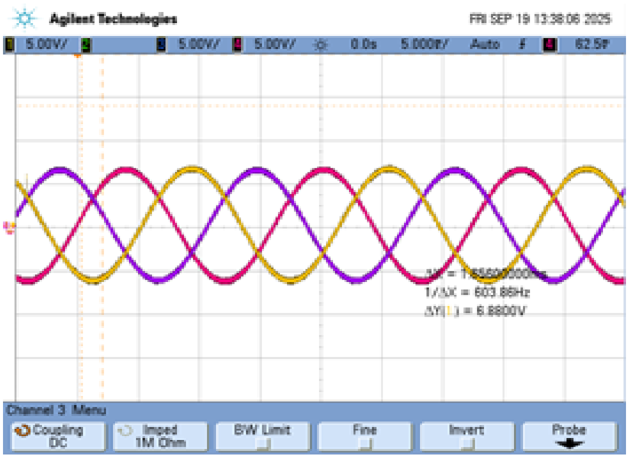

Fig.2 (b) Three-phase OP-AMP output voltage wave form shifted by 120°.

Triangular wave-form generator

The integrated circuit precision waveform generator is used to generate a 1 kHz triangular waveform by connecting the required resistor and capacitor. It is required to modulate the sine wave voltage to get PWM waveform[3],[4]. The triangular waveform is shown in the Fig. 2(c).

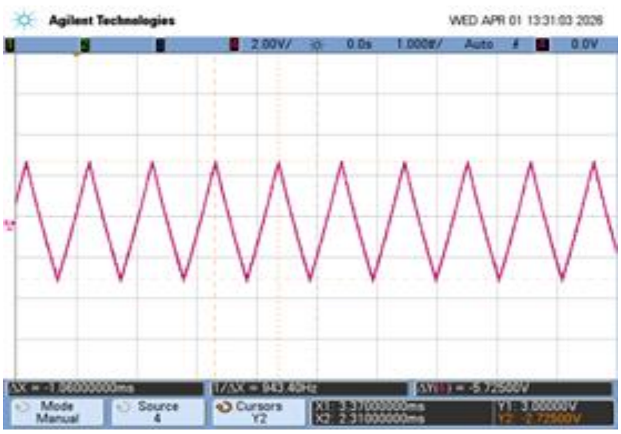

Fig.2(c) Triangular waveform.

Pulse Width Modulation

The output voltages sine waveform and the triangular waveform are summed up and amplified by using the integrated circuit chip (precision operational amplifier) are particularly suited for high source impedance and low

DOI: 10.46121/pspc.54.3.32

power dissipation [2]. In the same way, all three phases are done, and the three phase PWM[4] output of the amplifier is shown in Fig.2 (d).

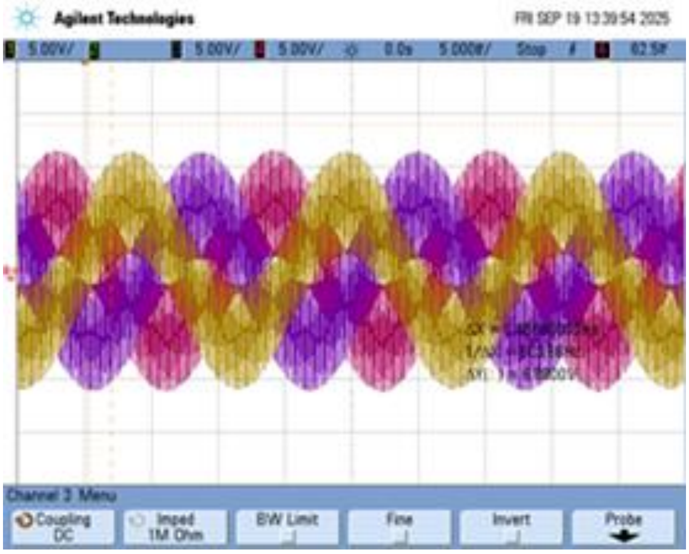

Fig.2 (d). Three-phase PWM output voltage waveform.

Current Transformer

The disc type ferrite core is used for the current transformer. The inverter output is passed through the current transformer to the three phase induction motor terminals. The CT is used for the feed back to the comparator. The secondary winding is shorted by an appropriate resistor. Similarly, all three phases are connected in a star configuration. The star point is connected to the ground terminals. All three phases of secondary output voltages are amplified by OPAMP.

Comparator

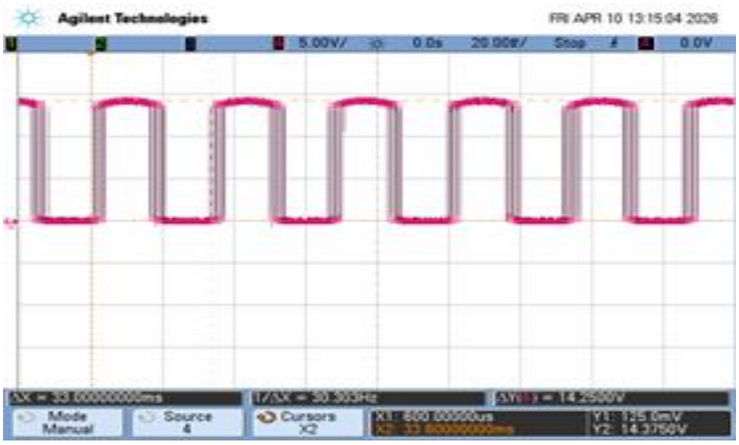

Fig. 2(e). Comparator output voltage

The single high speed voltage comparator IC compares the PWM output voltage and the current transformer secondary respective amplified phase feedback voltage. The difference is then amplified and the required pull-up resistor is connected to appropriate terminal to +15V. The comparator output voltage is shown in Fig.2 (e).

CMOS Low Power Astable Multivibrator

An astable multivibrator with a frequency of ~10kHz with an appropriate resistor and capacitor combination. This particular IC is used to achieve a stable oscillation frequency as shown in Fig. 2(f). The output is taken from the output terminal of the IC. Since it is used to block transient pulses of more than ~10 kHz to enter the inverter model.

DOI: 10.46121/pspc.54.3.32

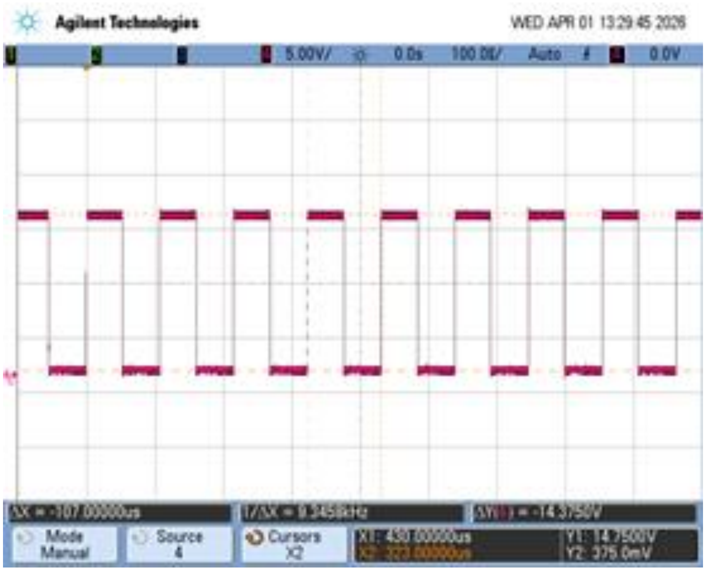

Fig.2 (f) Astable-Multivibrator

CMOS Dual D-type Flip-Flop.

This is used to get a complementary output voltage, which is required to enable the MOSFET of the same leg at the inverter block.

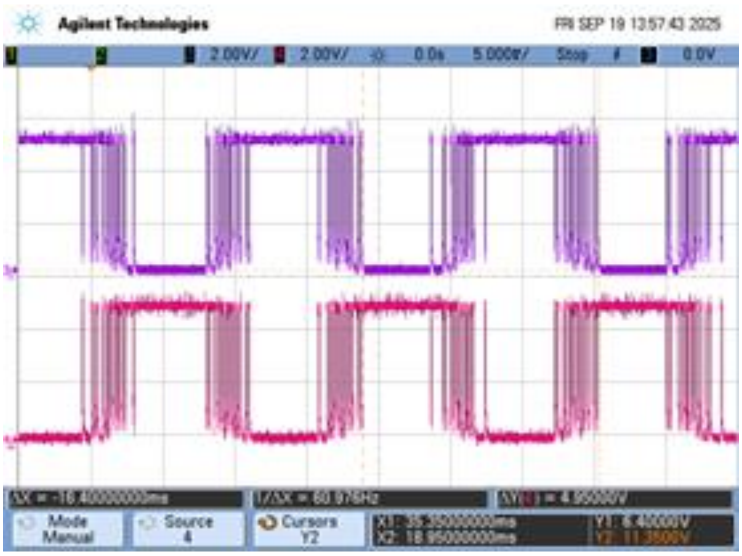

Fig. 2(g). Buffered, level-shifted (+5V) voltage for one leg.

The output voltage of the comparator and the Astable multivibrator are fed to this IC, and the complementary output voltage is taken from the appropriate terminals of the IC. Similarly, for all three phases, the voltages will be applied with the corresponding IC's. These complementary voltages are buffered and shifted to a 5V level, as shown in Fig.2(g).

Dead zone generator and opto-coupler

To avoid shoot-through in the inverter legs, a dead zone is introduced using the cmos AND gate with necessary resistor and capacitor. The dead zone generator output is coupled by using the opto-coupler. The necessary isolated power supply is introduced for the opto-couplers. The opto-coupler output of one of the phases of one leg is shown in Fig.2(h). The optocoupler output is connected to the corresponding gates of the 3-phase inverter devices.

DOI: 10.46121/pspc.54.3.32

Power System Protection and Control
ISSN:1674-3415

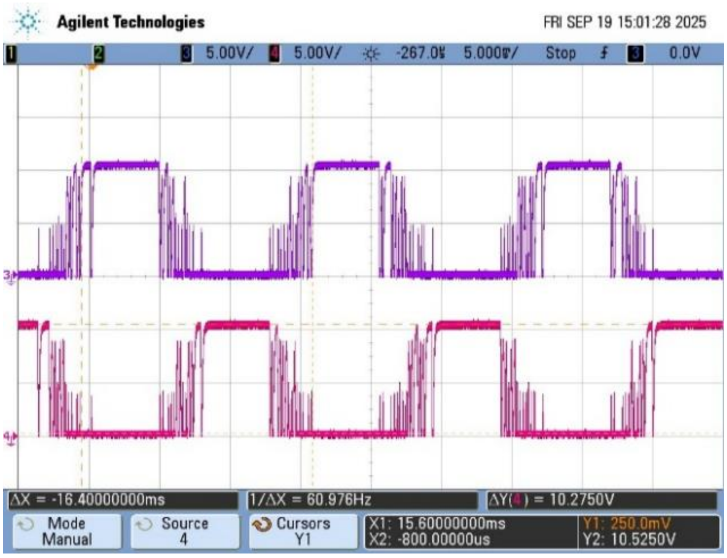

Fig. 2(h). Opto-coupler output for one leg.

Three-phase Inverter Bridge

Six Power MOSFETs are used for the inverter bridge with a suitable Undeland snubber circuit to protect the inverter devices [3], [5], [7]. The typical output voltage waveforms of phase, line, and snubber inductor voltages are shown in Fig.2 (i).

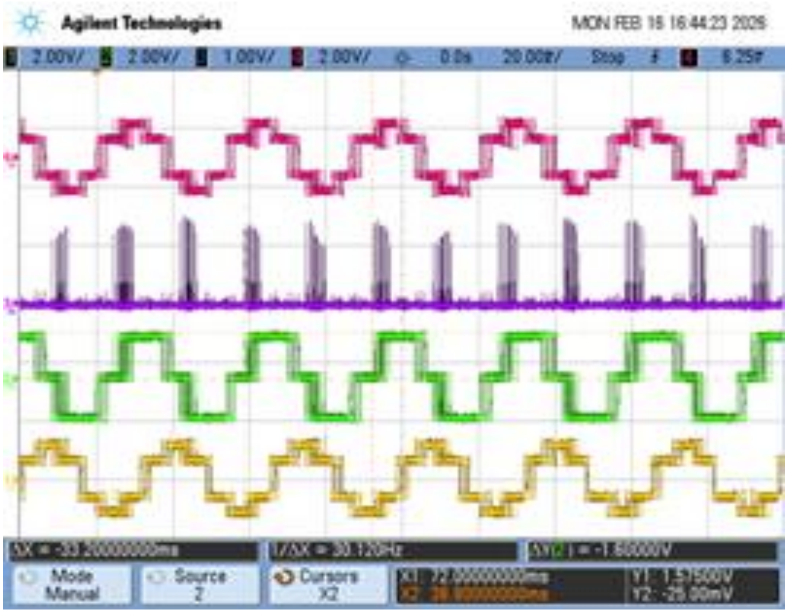

Fig. 2(i). Ch1: Phase voltage, 200:1, Ch2: line voltage, 250:1, Ch3: across inductor voltage, 25:1, Ch4: Phase voltage, 200:1.

RESULTS AND CONCLUSION

The motor terminal voltages are shown in Fig.2(i), and there is no overshoot of voltages. The phase and the line voltages are clear. With the proper Undeland snubber components the waveforms are perfect. The system is tested with frequencies of 30, 40, 50, 60 and 62.5Hz. The motor terminal voltages also stored in CSV format and this can be used to do FFT by using the Origin signal analysis software. Which can be validated from the math function FFT results of the (MSO) mixed signal oscilloscope. The FFT gives the results in frequency domain, hence the amplitude of fundamental and the higher order harmonic frequency component values can be obtained. The frequency domain results can be used to minimize the voltage values of higher harmonic order frequency, since

DOI: 10.46121/pspc.54.3.32

these frequencies may develop negative torque and heat, which will weaken the insulation of the winding of the motor and also may produce EMI which may disturb measuring instruments/equipment and sensing devices.

ACKNOWLEDGEMENT

The authors are thankful to the KRJS management for providing the facilities and funds to do the experimental work. The authors are also thankful to the Principal, Vice Principal, and HOD of the ECE department for their cooperation and permission to conduct the experimental work. The authors are thankful to Mr. R. Narayanan B.E, M.S for suggesting the various components in the blocks of control system design and the testing methods for the experimental work.

REFERENCES

1. Akire Nabae, Kenichi Otsuka, H Uchino, R Kurosawa, “An approach to flux control of IM operated with variable frequency supply”, IEEE trans industry applications, Vol.IA-16, PP.342-350, issue 3 May 1990.
2. A Nabae, I. Takahashi, and H Akagi, “A new neutral-point clamped PWM inverter”, IEEE trans. IND. Applications, Vol.IA-17, PP.518-523, Sep/Oct 1981.
3. A Ramachandran, M Channa Reddy, “Noval method of mitigation of conducted EMI in PWM inverter fed IM adjustable speed drives”, IEEE international conference on Industrial technology, ICIT-Dec, 15-17, 2006 held at Mumbai, India.
4. G Narayan and V T Ranganathan “Synchronized PWM strategies based on space vector approach principles of waveform generation”, IEEE proceedings-Electric power applications, Vol.146 No.3, May 1999, PP.267-275.
5. Julian Camargo Lopez, Oscar David Florez Cediel and Johann Hernandez Mora, “A Low-cost Adjustable Speed Drive for Three Phase Induction Motor”, 2017 IEEE Workshop on Power Electronics and Power Quality Applications (PEPQA), 17 July 2017.
6. M. Rashid, Power Electronics Handbook, Academic Press. 2001
7. Chen, Q., et al. "PV Integration with Low-THD SiC Inverters." Solar Energy Journal, 2021.
8. Agrawal, Gopal, Harshit Mohan, and Mukesh Pathak. "Improved Speed Sensorless Control of Induction Motor Drive Using Artificial Neural Network." 2022 2nd International Conference on Power Electronics & IoT Applications in Renewable Energy and its Control (PARC). IEEE, 2022.
9. S. Laha, J. Dhali and P. K. Gayen, "Comparative Performance between V/F and Rotor Flux-Oriented Controls of Induction Motor Drive," 2023 IEEE Devices for Integrated Circuit (DevIC), Kalyani, India, 2023, pp. 1-6, doi: 10.1109/DevIC57758.2023.10134999.
10. S. Kim, I. Yoon, C. Hong, J. Ko and S. Oh, "A study on a new sensorless control method for an induction motor using a non-linear speed observer and hybrid V/f control method," 2023 IEEE Texas Power and Energy Conference (TPEC), College Station, TX, USA, 2023, pp. 1-5, doi: 10.1109/TPEC56611.2023.10078673
11. Anurag D Jangde, Khushal J Bhajipale, Shrey S Potbhare, “Speed Controlling of Three-Phase Induction Motor Using VFD”, April 2024, IJIRT, Volume 10 Issue 11, ISSN: 2349-6002.
12. Janvhi Shukla, Mahak Pal, Priya Lacharwar, Rutuja Agashe, Saloni Bhoskar. “Speed Control of Three-Phase Induction Motor Using Advance Controller “, International Open-Access, Double-Blind, Peer-Reviewed, Refereed, Multidisciplinary Online Journal Volume 6, Issue 3, April 2026